J. Comput. Appl. Res. Mech. Eng. Vol. 13. No. 1, pp. 67-74, 2023 *DOI: 10.22061/JCARME.2023.9454.2270*

SRTTU

Journal of Computational and Applied Research in Mechanical Engineering

jcarme.sru.ac.ir

JCARME

ISSN: 2228-7922

Research paper

Lattice Boltzmann simulation inside a cavity: The effect of pipe profile on natural convection

Seyed Mostafa Moafi Madani, Javad Alinejad* , Yasser Rostamiyan and Keivan Fallah

Department of mechanical engineering, Sari branch, Islamic Azad University, Sari, Iran

Article info:

Article history:

Received: 03/12/2022

Accepted: 25/04/2023

Revised: 27/04/2023

Online: 29/04/2023

Keywords:

Lattice Boltzmann model,

Fuel heating,

Particle volume fraction,

Two–phase fluid,

Natural convection.

***Corresponding author:**

Alinejad_javad@iausari.ac.ir

Abstract

In the present study, the effect of the heating pipe profile on natural convection in a two-phase fluid inside a cavity has been investigated. This geometry has been simulated with the LB Method based on the D2Q9 model for analyzing stream lines, dimensionless velocity field of fluid flow, solid particles volume fraction, temperature arrangement, and Nusselt number. These parameters have been studied in three different cases of the cavity. The results are signified by changing the geometry from a horizontal ellipse to a circular one and a vertical ellipse;the maximum particle volume fraction is decreased. Also, by changing the geometry from a horizontal ellipse to a circular and vertical ellipse, larger velocity vectors have been formed around the geometry. The Nusselt number variations of circular and vertical ellipse geometries are from 90º to 270º. The Nusselt number variation of horizontal ellipse geometry is negligible from 90º to 270º. Also, the Nusselt number of the circular geometry is larger than the other geometries from 270º to 90º. The highest average Nusselt number belongs to circular, vertical and horizontal ellipse geometries, respectively.

1. Introduction

Problems of heating fuel storage tanks are always one of the main challenges of the industry. Temperature arrangement, maintaining thermal efficiency and reducing energy loss, and preventing the deposition of suspended solid particles are important issues in this field. On the other hand, gravity causes particles to deposit on surfaces. Over time and with the increase of sediment, the heat transfer rate will decrease. As a result, efficiency is reduced, and fuel consumption increases. Of course, the system to be fueled is very important in determining the conditions of fuel and storage tanks. Therefore, the simulation of fuel tanks and heating systems will be very useful to reduce energy consumption and costs.

To simulate the fuel storage tank, it can be considered as a cavity with a heating system that different methods have been used by researchers. Esfahani and Alinejad [1] investigated the flow rate and heat transfer effects in a chamber with a movable wall by the LB method. Esfahani and Alinejad [2] simulated the effect of entropy production in a cavity by LBM. Alinejad *et al.*

[3] investigated the effect of force convection on multiple baffles by the LB method. Alinejad *et al.* [4] simulated the effects of free convection on cylinders with LBM. Esfahani *et al.* [5] investigated the effects of free convection on particles by the LB method. Alinejad and Fallah [6] simulated the heat transfer of the nanofluid in an enclosure. Alinejad *et al.* [7] investigated a three-dimensional model in a cavity by LBM. Maddah *et al.* [8] investigated the nanofluid effect and fins layout on heat transfer in a cavity. Peiravi *et al.* [9] studied heat transfer in a channel by the LB method. Peiravi *et al.* [10] simulated the effect of the nanofluid on convection in a cavity by LBM. Wang *et al.* [11] investigated the precipitation of petroleum. They reported the impossibility of providing an empirical relationship for the precipitation. Also, the error of extracted equations is very high and non-negligible. Haghshenasfard and Hooman [12] investigated the sedimentation rate of exchangers. They found that different parameters affect the amount of precipitation. Eventually, they compared the results with the measured data. He and Wang [13] studied the effect of particle attachment in turbulent conditions and the effect of large eddies on the modeling of particle dispersion and deposition without considering the effects of the particles on the field and other particles to determine the path particles numerically. Kor and Kharrat [14] investigated the flow characteristic of the sedimentation. The drag force on the solid boundary declined. Seyyedbagheri and Mirzayi [15] carried out a 3D model. Thespeed of sedimentation in a turbulent flow was studied. Emani et al. [16] numerically investigated the effect of the tension on sedimentation in exchangers. They reported a negligible fluctuation of the precipitation when the shear force was increased. Peiravi and Alinejad [17] investigated the diffusion of particles in a chamber with installed barriers. Abbassi *et al.* [18] investigated the heat transfer in garbage incinerators. Safaei *et al.* [19] simulated the natural convection of nanofluid in a chamber by LB modeling. Goodarzi *et al.* [20] investigated the moving lid enclosure with LBM.Zhou *et al.* [21] simulated the convection of nanofluid in a chamber. Shaker *et al.* [22] investigated the effect of a magnetic field on mixed convection inside an enclosure. The result of this study shows the positive effect of a significant increase in the Nusselt number with an increase in the magnetic number. Zhang *et al.* [23] investigated the natural convection melting in a chamber with a heat source. They observed the change in melting time by moving the cylinder. Rajarathinam *et al.* [24] investigated the convection of nanofluid in a chamber. The result of their study shows that the movable wall is affected by the flow. Alsabery *et al.* [25] investigated the free convection of nanofluid in an enclosure. Jamesahar *et al.* [26] investigated the particles and fluid interaction in free convection in a chamber.

In the present study, the effects of the profile of heating pipes on the natural convection of two-phase flow are investigated. These cases are simulated with the LBM based on a two-dimensional model and studied in 3 cases of the fuel tank with different profiles of floor heating pipes. The simulation in this method is Fortran Software.

2. Problem definition

The profile of heating pipes' effects on the stream lines, dimensionless velocity field of fluid flow, temperature arrangement, Nusselt number, and distribution of suspended particles in cavities is presented. The dimensions of the shape, boundary conditions, and different profiles of heating pipes in 3 cases of the fuel heating tank are illustrated in Fig. 1. The profile of heating pipes is simulated at an equal cross-section. Except for the lower wall where the temperature is constant, other walls are adiabatic.

3. Simulation methodology

3.1. Lattice Boltzmann Method

In CFD simulation, the governing equations of two-phase flow (continuity, momentum, energy) are expressed as follows:

$$\nabla.\vec{V} = 0 \quad (1)$$

$$\rho\frac{D\vec{V}}{Dt} = -\nabla p + \rho\vec{g} + \mu\nabla^2\vec{v} \quad (2)$$

$$\rho\frac{Dh}{Dt} = \frac{Dp}{Dt} + div(k\nabla T) + \emptyset \quad (3)$$

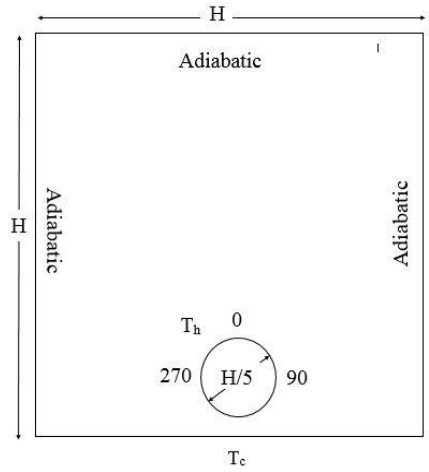

Case 1: Circular

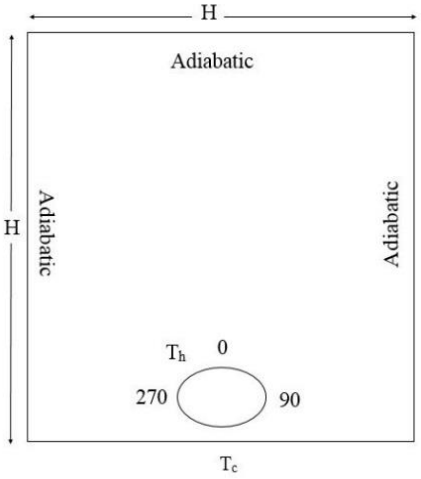

Case 2: Horizontal elliptic

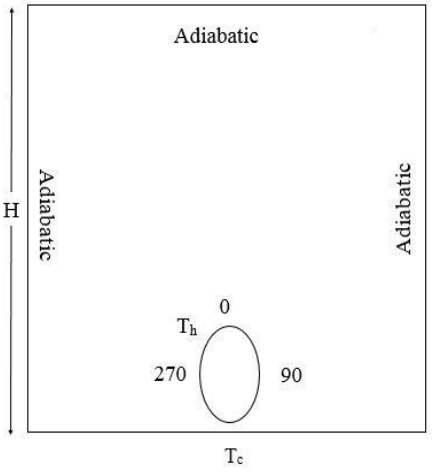

Case 3: Vertical elliptic

Fig. 1. Fuel heating tanks schematics and boundary conditions

The Lattice Boltzmann model is based on a mesoscopic view and is different from CFD models. Variety of Lattice Boltzmann methods dependent on the number of velocity vectors. In this work, a fuel heating tank with nine velocity vectors ($c_0 \dots c_8$), in two-dimension is illustrated in Fig. 2, where I and $c = \Delta x/\Delta t$ are direction of Lattice velocities. By solving the LBE, the DFs are obtained. It is a discretization of the LB equation. The multi-phase BE is as follows [27]:

$$f_i^{\sigma}(\mathrm{x} + \mathrm{e}_i\Delta t,\, t{+}\Delta t) - f_i^{\sigma}(\mathrm{x},\, t)$$

$$= -\frac{1}{\tau^{\sigma}}\left(f_i^{\sigma}(\mathrm{x},\, t) - f_i^{\sigma,eq}(\mathrm{x},\, t)\right)$$

$$+\left(\frac{2\tau^{\sigma}-1}{2\tau^{\sigma}}\right)\left(\frac{F_i^{\sigma}\cdot \mathrm{e}_i\Delta t}{B_i c^2}\right) + \Delta t F_i \qquad (4)$$

where $\sigma = 1\ 2$ are the indicator of each component and τ_f^{σ} is the relaxation time and e_i is the ith direction of velocity vector. Also, $f_i^{\sigma,eq}$ is the particle equilibrium distribution function which is related to the movement *ith* direction in the velocity space. The equilibrium density distribution functions of the *σth* component, $f_i^{\sigma,eq}$ in two-dimensional space are as follows:

$$f_i^{\sigma,eq}(x,t) = \omega_i \rho^{\sigma}\left[1 + \frac{3e_i\cdot u^{\sigma,eq}}{c^2} + \frac{9(e_i\cdot u^{\sigma,eq})^2}{2c^4} - \frac{3(u^{\sigma,eq})^2}{2c^2}\right] \qquad (5)$$

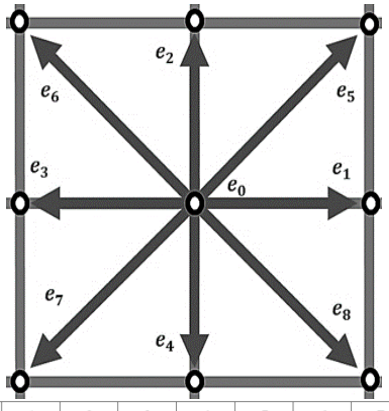

i	0	1	2	3	4	5	6	7	8
c_i	(0,0)	(1,0)c	(0,1)c	(-1,0)c	(0,-1)c	(1,1)c	(-1,1)c	(-1,-1)c	(1,-1)c

Fig. 2. Two-dimensional model of velocity lattice.

Also, δx is the lattice space and δt is the lattice time step. They are taken as unity and their ratio $= \delta x/\delta t$. The macroscopic density, kinematic viscosity and velocity of the σth component are given by $\rho^{\sigma}(x,t) = \sum_i f_i^{\sigma}(x,t)$, $\nu^{\sigma} = \left(2\tau_f^{\sigma} - 1/6\right)c^2\Delta t$ and $u^{\sigma} = \sum_i f_i^{\sigma}(x,t)e_i$ respectively. In this equation, the equilibrium velocities$u^{\sigma,eq}$ is calculated as follows:

$$u^{\sigma,eq} = \frac{1}{\rho^{\sigma}}\sum_i f_i^{\sigma} e_i + \frac{F^{\sigma}\tau_f^{\sigma}\Delta t}{\rho^{\sigma}} \quad (6)$$

Similarly, the thermal equation is calculated as follows:

$$g_i^{\sigma}(x + e_i\Delta t, t+\Delta t) - g_i^{\sigma}(x, t) = -\frac{1}{\tau^{\sigma}}\left(g_i^{\sigma}(x, t) - g_i^{\sigma,eq}(x, t)\right) \quad (7)$$

where g_i^{σ} is the ith energy distribution function and τ^{σ} is the thermal relaxation time of the component. The energy equilibrium distribution functions are calculated as follows:

$$g_i^{\sigma,eq}(x,t) = \omega_i\theta^{\sigma}\left[1 + \frac{3e_i\cdot u^{\sigma,eq}}{c^2} + \frac{9(e_i\cdot u^{\sigma,eq})^2}{2c^4} - \frac{3(u^{\sigma,eq})^2}{2c^2}\right] \quad 8$$

Finally, the macroscopic temperature is calculated as follows [27]:

$$T = \sum g_k \quad (9)$$

The weight values of each velocity vectors are shown in Table 1.

In the present work, the applied forces between fluid and solid particles are Brownian, gravity and drag forces.

So, based on stokes law, the drag force applied on the suspend particles is calculated as follows:

$$F_D = 3\pi\mu d_p(V - V_P) \quad (10)$$

Table 1. The weight values of velocity vectors.

i	1	2	3	4	5	6	7	8	9
W_i	$\frac{4}{9}$	$\frac{1}{9}$	$\frac{1}{9}$	$\frac{1}{9}$	$\frac{1}{9}$	$\frac{1}{36}$	$\frac{1}{36}$	$\frac{1}{36}$	$\frac{1}{36}$

where, V is the fluid velocity and V_p is the suspend particles velocity. The force of the gravity is calculated as follows [27]:

$$F_G = -\frac{\pi(d_p)^3 g\Delta\rho}{6} \quad (11)$$

where d_p is solid particles diameter and $\Delta\rho$ is a mass density difference between two components. The Brownian force applied on the suspend particles is calculated as follows [27]: (3)

$$F_B = c_B\frac{2k_BT}{d_p} \quad (12)$$

where, C_B is the Brownian diffusion coefficient. This is equal to 1×10^{14} for spherical particles. K_B is the Boltzmann constant and T is the absolute temperature of base fluid.

4. Validation for LBM

In this section, the LBM simulation and reference results are compared. In Fig. 3, the variation of dispensation of solid particles in a cavity is compared with the research of Ahmed and Eslamian [27]. There is an acceptable match between the results of this work and the reference data.

5. Results and discussion

In this study, three different cases of the fuel tank with various profiles of heating pipes are investigated. The Characteristics of particles and fluid are shown in Table 2.

Fig. 4 shows the stream lines in each cavity. In all three cases, the stream lines are formed around the center between the profiles and the side walls. The direction of movement is such that the flow comes down from the side walls and then moves upwards parallel to the geometries and in the center of the cavities. By comparing the stream lines, it can be seen that by changing the geometry from a horizontal ellipse to a circular and vertical ellipse, the stream lines near the profile become closer, which indicates that the velocity is increased.

Table 2. Characteristics of particles and fluid.

Material	Density (Kg/m^3)	Viscosity (m^2/s)
Oil	870	1.07×10^{-5}
Particle	8940	7.0×10^{-5}

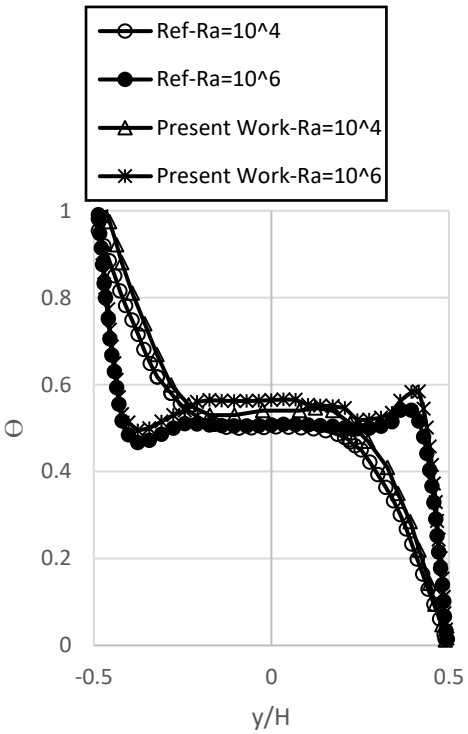

Fig. 3. Comparison between the present study and reference results.

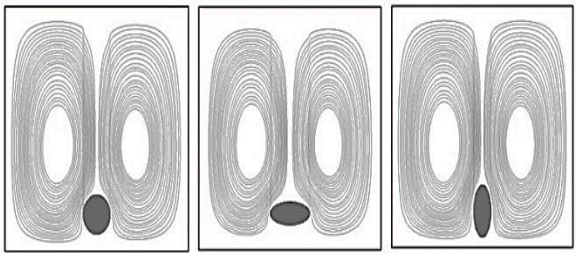

Fig. 4. Comparison between streamlines.

Fig. 5 illustrates the dimensionless velocity contours in the cavities. The rotating path formed on both sides of the profiles. In all of the cases, the flow passed through the same path whereas the stream line near the profile was different. By changing the geometry from a horizontal ellipse to a circular and vertical ellipse, a larger velocity was created over the profile.

Dispersion of suspended solid particles for three cases is shown in Fig. 6. As shown in the picture, by changing the geometry from vertical ellipse to circular and horizontal ellipse, the volume fraction of solid particles and the thickness of the layer on the profile increases. Also, for all three cases, the distribution of particles in the middle of the profile and the upper wall is the same.

In Fig. 7, the temperature arrangement of each cavity is illustrated. In the cavity with circular geometry, the upper wall has three temperature ranges, but in other two cavities, this wall is completely isothermal.

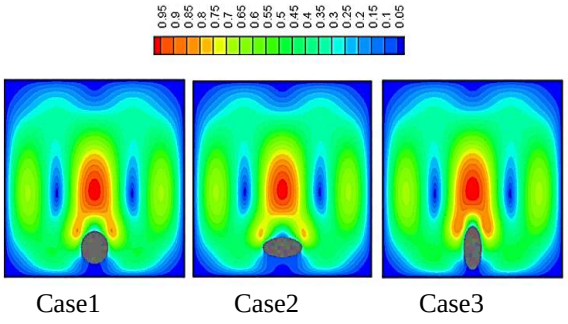

Fig. 5. Comparison of dimensionless velocity.

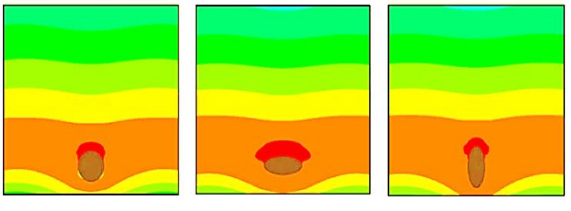

Fig. 6. Comparison dispersion of suspended solid particles.

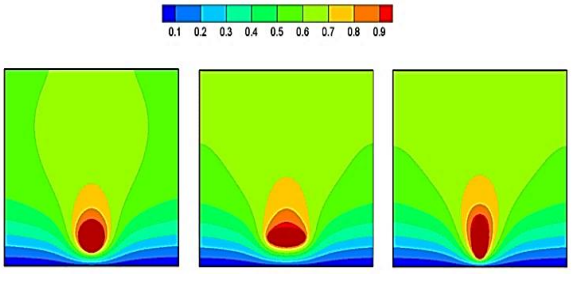

Fig. 7. Comparison of the dimensionless temperature arrangement.

Fig. 8 shows the changes of Nusselt number of circular and horizontal and vertical ellipse geometries. The maximum Nusselt number of the circular and vertical ellipse geometries are at angle of 180 degrees. The vertical ellipse and circular geometry have a similar behavior from angle of 60 degree to 330 degree. Its maximum Nusselt number is equal to 72% of the circular geometry. But the behavior of the horizontal ellipse is different from the other two geometries. The changes of the Nusselt number on the lower surface of the horizontal ellipse are negligible. Also, the changes of the Nusselt number on the upper surface of the circular geometry are insignificant compared to other geometries. Based on three geometries, the minimum Nusselt number rises at angle of 30 degrees, at this point the Nusselt numbers for vertical and horizontal ellipse geometries have the same value and are equal to 56% of the Nusselt of circular geometry. The maximum Nusselt number of the horizontal ellipse geometry, which is between 70 and 108 angles, is higher than the Nusselt number of the circular and vertical ellipse geometry in that area, respectively. The average Nusselt number of circular, vertical ellipse and horizontal ellipse geometries are equal to 37.94, 28.76 and 25.58, respectively.

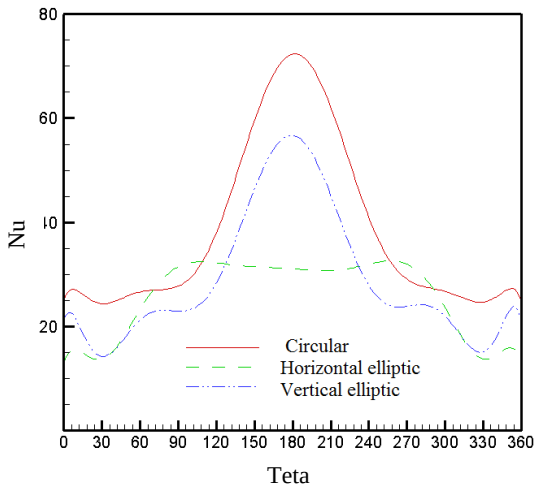

Fig. 8. Comparison of Nusselt number on the environment of geometries.

5. Conclusions

In this study, three cases of the cavity with different profiles of heating pipes were investigated. Also, the profile change of the tubes effects on stream lines, dimensionless velocity field of fluid flow, solid particles volume fraction, temperature arrangement and Nusselt number with two-dimensional model of Boltzmann method were simulated. Eventually, some of the most important points are summarized below:

- Based on three cases, the Maximum volume fraction of solid particles in horizontal ellipse is the highest. In addition, the volume fraction of the circular is more than that of the vertical ellipse shape.
- The average Nusselt number increases from a horizontal ellipse geometry to a circular geometry. Also, in a horizontal ellipse geometry, the average Nusselt number increases by moving away from the angle of 180 degrees, whereas this difference is less than 1%. Furthermore, the Nusselt number of the vertical and the horizontal ellipse geometries have the same value. It is around 56% of the circular geometry.

References

[1] J. Esfahani and J. Alinejad, "Lattice Boltzmann simulation of viscous-fluid flow and conjugate heat transfer in a rectangular cavity with a heated moving wall," *Thermophys. Aeromech.*, Vol. 20, No. 5, pp. 613-620, (2013).

[2] J. Esfahani and J. Alinejad, "Entropy generation of conjugate natural convection in enclusures: The Lattice Boltzmann method," *J. Thermophys. Heat Transfer*, Vol. 27, No. 3, pp. 498-505, P. 07/01, (2013).

[3] J. Alinejad and J. A. Esfahani, "Lattice Boltzmann simulation of forced convection over an electronic board with multiple obstacles," *Heat Transfer Res.*, Vol. 45, No. 3, pp. 241-262, (2014).

[ ] J. Alinejad and J. Abolfazli Esfahani, "Numerical stabilization of three-dimensional turbulent natural convection around isothermal

cylinder," *J. Thermophys. Heat Transfer*, Vol. 30, No. 1, pp. 94-102, (2016).

[5] J. Alinejad and J. Esfahani, "Lattice Boltzmann simulation of EGM and solid particle trajectory due to conjugate natural convection," *Aerospace. Sci. Technol*; Vol. 4. No. 1, pp. 36–43. (2016).

[6] J. Alinejad and K. Fallah, "Taguchi optimization approach for three-dimensional nanofluid natural convection in a transformable enclosure," *J. Thermophys. Heat Transfer*, Vol. 31, No. 1, pp. 1-7 (2016).

[7] J. Alinejad and J. A. Esfahani, "Taguchi design of three dimensional simulations for optimization of turbulent mixed convection in a cavity," *Meccanica*,Vol. 52, No. 4, pp. 925-938, (2017).

[8] M. M. Peiravi, J. Alinejad, D. Ganji and S. Maddah, "Numerical study of fins arrangement and nanofluids effects on three-dimensional natural convection in the cubical enclosure," *Challenges Nano. Micro. Scale. Sci. Technol.*, Vol. 7, No. 2, pp. 97-112, (2019).

[9] M. M. Peiravi and J. Alinejad, "Hybrid conduction, convection and radiation heat transfer simulation in a channel with rectangular cylinder," *J. Therm. Anal. Calorim*,Vol. 140, No. 6, pp. 2733-2747, (2020).

[10] M. M. Peiravi, J. Alinejad, D. D. Ganji, and S. Maddah, "3D optimization of baffle arrangement in a multi-phase nanofluid natural convection based on numerical simulation," *Int. J. Numer. Methods Heat Fluid Flow*, Vol. 30, No. 5, pp. 2583-2605, (2019).

[11] Y. Wang, Z. Yuan, Y. Liang, Y. Xie, X. Chen and X. Li, "A review of experimental measurement and prediction models of crude oil fouling rate in crude refinery preheat trains," *Asia-Pac. J. Chem. Eng.*,Vol. 10, No. 4, pp. 607-625, (2015).

[12] M. Haghshenasfard and K. Hooman, "CFD modeling of asphaltene deposition rate from crude oil," *J. Petrol. Sci. Eng.*, Vol. 128, pp. 24-32, (2015).

[13] S. D. He and B. Wang, "Dispersion of particles in wall-bounded particle-laden turbulent flows with high wall permeability," *Int .J. Multiph. Flow*, Vol. 77, No. 4, pp. 104-119, (2015).

[14] P. Kor and R. Kharrat, "Modeling of asphaltene particle deposition from turbulent oil flow in tubing: Model validation and a parametric study," *Petrol.*, Vol. 2, No. 4, pp. 393-398, (2016).

[15] H. Seyyedbagheri and B. Mirzayi, "CFD modeling of high inertia asphaltene aggregates deposition in 3D turbulent oil production wells, *J. Petrol. Sci. Eng.*",Vol. 150, pp. 257-264, (2017).

[16] S. Emani, M. Ramasamy and K. Z. K. Shaari, "CFD modelling of shell-side asphaltenes deposition in a shell and tube heat exchanger," *AIP Conference Proceedings*, Vol. 1859, No. 1: AIP Publishing LLC, p. 020118, (2017).

[17] M. M. Peiravi and J. Alinejad, "Nano particles distribution characteristics in multi-phase heat transfer between 3D cubical enclosures mounted obstacles," *Alexandria Eng. J.*, Vol. 60, No. 6, pp. 5025-5038, (2021).

[18] M. A. Abbassi, M. R. Safaei, R. Djebali, K. Guedri, B. Zeghmati and A. A. Alrashed, "LBM simulation of free convection in a nanofluid filled incinerator containing a hot block," *Int. J. Mech. Sci.*, Vol. 144, pp. 172-185, (2018).

[19] M. R. Safaei, A. Karimipour, A. Abdollahi and T. K. Nguyen, "The investigation of thermal radiation and free convection heat transfer mechanisms of nanofluid inside a shallow cavity by lattice Boltzmann method," *Physica A*, Vol. 509, pp. 515-535, (2018).

[20] M. Goodarzi, A. D'Orazio, A. Keshavarzi, S. Mousavi and A. Karimipour, "Develop the nano scale method of lattice Boltzmann to predict the fluid flow and heat transfer of air in

the inclined lid driven cavity with a large heat source inside, Two case studies: Pure natural convection & mixed convection," *Physica A*, Vol. 509, pp. 210-233, (2018).

[21] X. Zhou, F. Chi, Y. Jiang and Q. Chen, "Numerical investigation of thermocapillary convection instability for large Prandtl number nanofluid in rectangular cavity," *Int. Commun. Heat Mass Transfer*, Vol. 133, p. 105956, (2022).

[22] H. Shaker, M. Abbasalizadeh, S. Khalilarya, and S. Yekani Motlagh, "Two-phase modeling of the effect of non-uniform magnetic field on mixed convection of magnetic nanofluid inside an open cavity, " *Int. J. Mech. Sci*, Vol. 207, 106666, (2021).

[23] X. Zhang, L. Wang, and D. Li, "Lattice Boltzmann simulation of natural convection melting in a cubic cavity with an internal cylindrical heat source," *Int. J. Therm*. Sci, Vol. 165, p. 106917, (2021).

[24] M. Rajarathinam, N. Nithyadevi and A. J. Chamkha, "Heat transfer enhancement of mixed convection in an inclined porous cavity using Cu-water nanofluid," *Adv. Powder Technol*., Vol. 29, No. 3, pp. 590-605, (2018).

[25] A. Alsabery, M. Sheremet, A. Chamkha, and I. Hashim, "Conjugate natural convection of Al_2O_3–water nanofluid in a square cavity with a concentric solid insert using Buongiorno's two-phase model, " *Int. J. Mech. Sci*, Vol. 136, pp. 200-219, (2018).

[26] E. Jamesahar, M. Ghalambaz, and A. Chamkha, "Fluid–solid interaction in natural convection heat transfer in a square cavity with a perfectly thermal-conductive flexible diagonal partition," *Int. J. Heat Mass Transfer*,Vol. 100, pp. 303-319, (2016).

[27] M. Ahmed and M. Eslamian, "Natural convection in a differentially-heated square enclosure filled with a nanofluid: significance of the thermophoresis force and slip/drift velocity," *Int. Commun. Heat Mass Transfer*, Vol. 58, pp. 1-11, (2014).

How to cite this paper:

Seyed Mostafa Moafi Madani, Javad Alinejad, Yasser Rostamiyan and Keivan Fallah, "Lattice Boltzmann simulation inside a cavity: The effect of pipe profile on natural convection,", *J. Comput. Appl. Res. Mech. Eng.*, Vol. 13, No. 1, pp. 67-74, (2023).

DOI: 10.22061/JCARME.2023.9454.2270

URL: https://jcarme.sru.ac.ir/?_action=showPDF&article=1873